energy&fuels

Article

pubs.acs.org/EF

Characteristics of the Temperature Distribution and Product Gas Evolving of an Updraft Biomass Gasifier

Bin Li, Hanping Chen, Haiping Yang,* Xianhua Wang, and Shihong Zhang

State Key Laboratory of Coal Combustion, Huazhong University of Science and Technology, Wuhan, 430074, China

ABSTRACT: This paper aims to reveal the temporal and spatial variation of temperature and product gas components inside the updraft biomass gasifier, and the relationship between it and the chemical reaction was also analyzed. Using wood processing residues, the gasification characteristics of the gasifier were studied in depth. The results indicated that the gas products could be ignited after the gasifier startup 4 min and the time of normal operation condition was 81 min. The optimum air flow rate of the gasifier was ~1.9 m^3/h, with a LHV of product gas of 4.38 MJ/Nm^3, temperature of the oxidation zone of 960 °C, and gasification intensity of 57.8 $kg/(m^2 \cdot h)$. Along with the height direction, the layered characteristic of reaction type was very obvious, and the height of the oxidation zone, reduction zone, pyrolysis zone, and desiccation zone could be calculated approximately as 130 mm, 95 mm, 195 mm, and the rest of the material height, respectively.

1. INTRODUCTION

Energy, environment, and sustainable development are the main focuses in the world these days. The global energy resource is rather scarce, and environmental pollution caused by energy consumption is more and more serious. The current economic growth mode with the cost of consumption of energy and expense of the environment is unsustainable and must be changed.[1] Responding to the critical situation, the Chinese government proposes to build a resource-saving and environment-friendly society as an important breakthrough point and try to bring the development model onto a green, low-carbon, and sustainable track in the future. During the World Climate Conference in Copenhagen 2009, China made a solemn promise to the whole world: by 2020, China's energy consumption per unit of GDP would be reduced by 40−60% from the 2005 level, and the CO_2 emissions per unit of GDP would be cut by 40−45% from that in 2005.[2]

Considering that industry is the biggest department of energy consumption in China, which accounts for more than 70% of the total energy consumption, and the average thermal efficiency of China's large number of coal-fired industrial boilers and kilns is only 60−65%, their energy-saving and emission reduction is extremely urgent and also very important to achieve China's commitments.[3,4] Therefore, in China's "12th Five-Year Plan" of industrial energy saving, the energy-saving reformation of coal-fired boilers and kilns has been listed as the national 10 key energy-saving projects in the first place and technology upgrading, equipment renewal, and reformation is extremely urgent.[5]

As is known, biomass resource is a clean, renewable energy resource with the advantage of great production, wide distribution, and near-zero CO_2 net emission and its scale, and efficient and clean use for partial replacement of fossil fuels is one of the important ways for China to cope with the energy and environmental crisis and achieve energy savings, emission reduction, and sustainable development; it has been recognized unanimously and taken seriously by both the government and the business community. Combined with the current situation of China's coal-fired industrial boilers and kilns of fuel shortage, low efficiency, and serious pollution, using advanced biomass conversion and utilization technology to upgrade and reform the current coal-fired industrial boilers and kilns not only can make full use of the local cheap and abundant biomass resources, thus reducing dependence on coal supply, but also can change the industrial production process in a green, low-carbon, and efficient way, hence enhancing the enterprises' competence. Biomass gasification is one of the important choices for energy-saving reformation of coal-fired industrial boilers and kilns; it could easily covert low-grade biomass into high-grade combustible gas, thus providing heat to the industrial process via highly efficient and clean combustion, and the demands of the enterprise are growing significantly.

Nowadays, biomass gasifiers mainly include a fixed bed gasifier, fluidized bed gasifier, and entrained flow gasifier, etc. Different gasifiers have been used in different processes. Both a fluidized bed gasifier and entrained flow gasifier have higher gasification intensity per unit cross-section area and lower corresponding floor area relatively but a high cost of investment and complicated operation, which also leads to a high demand to the operator on the technical level. In addition, they are suitable for continuous operation and biomass large-scale utilization processes. While a fixed bed gasifier has the advantages of simple structure, low investment, convenient operation, and easy maintenance, it is easy to operate and has a fast speed of hot start; the running mode is flexible which can be not only continuous but also intermittent, which could be very suitable for the frequent starting and stopping industrial process; it has shown broad application needs. On the basis of this background, an updraft fixed bed biomass gasifier has been chosen as a combustible gas generator to make energy-saving reformation to the coal-fired industrial boilers and kilns. Moreover, the updraft biomass gasifier could also be used as a combustible gas generator in the central gas supply system in

Received: January 30, 2013
Revised: February 26, 2013
Published: February 28, 2013

dx.doi.org/10.1021/ef400176k | *Energy Fuels* 2013, 27, 1460−1465

some local regions or rural areas or maybe just a household occasion.

However, before that the gasification characteristics of the gasifier should be studied in depth. At present, there are already many practical industrial application facilities of the updraft biomass gasifier,[6,7] but relevant data reports and research literature are still very limited, especially about the temperature distribution and product gas evolving inside the gasifier.[8−11] The shortage on operation characteristics and reaction mechanism cause a severe dependence on experiences which is very unfavorable for optimal design and operation. Although much literature has been reported on coal gasifier studies,[12−14] considering the big difference between biomass and coal in physical properties (density and mobility, etc.) and chemical properties (composition, thermal conversion property, ash melting point, etc.),[15] the current results about a coal gasifier cannot be copied to use in a biomass gasifier. Therefore, in this study, we chose wood-processing residues as the raw material, and the gasification characteristics of an updraft gasifier were studied in depth. The temporal and spatial variation of the temperature and product gas components inside the gasifier were analyzed to reveal the mechanism of the gasification process, which could provide basic data and theoretical basis to optimal structural design and operation condition adjustment of the updraft biomass gasifier.

2. EXPERIMENTAL SECTION

2.1. Raw Material. The biomass material used here was pine wood processing residues. It is the mixture of pine wood block, pine wood shavings, and pine sawdust. Particle size was less than 5 cm. The low heating value (LHV) was measured using a bomb calorimeter (Parr 6300, Parr Instrument Co.). The proximate and ultimate analysis was analyzed using a TGA2000 (Las Navas, Spanish) and CHNS analyzer (EL-2, Vario Germany), respectively. Inorganic matter in wood sample was analyzed using X-ray fluorescence spectroscopy (XRF, EAGLE III, EDAX, Inc.) and shown on oxide basis as a percent of the ash mass. Ash fusibility was analyzed using the ash fusion test (Carbolite CAF). Relevant results are listed in Table 1. It can be observed that the wood material shows higher volatility and low N and S content with a higher LHV value of 16.46 MJ/kg. In addition, it also has a relatively higher ash content. It might be attributed to soil mixing, which also leads to a relatively higher content of Al and Fe in the ash.[16] Moreover, the ash fusion point of the wood ash is very low (~1100 °C).

Table 1. Physical and Chemical Properties of Pine Wood Sample

particle size (cm)	<5
stack density (g/cm^3)	0.11
low heating value (MJ/kg)	16.46
ultimate analysis (wt %, as received)	
C	45.37
N	0.29
O	34.01
H	6.96
S	0.51
proximate analysis (wt %, as received)	
fixed carbon	16.07
moisture	5.83
volatile	71.07
ash	7.03
ash component (on ash basis, wt %, by XRF)	
MgO	5.45
Al_2O_3	8.29
SiO_2	43.87
P_2O_5	3.12
SO_3	6.04
K_2O	6.97
CaO	17.97
TiO_2	0.76
Cr_2O_3	0.15
MnO_2	0.38
Fe_2O_3	6.24
CuO	0.06
ZnO	0.45
NiO	0.05
PbO_2	0.19
ash fusion point (°C)	
deformation temperature	1126
softening temperature	1170
flowing temperature	1194

2.2. Experimental Setup. Gasification experiments were performed in a lab-scale, autothermal updraft biomass gasifier, which is shown schematically in Figure 1. It is composed of several key parts: a gasifier proper system, an ignition system, an air distribution system, an ash handling system, and a temperature monitoring and gas sampling system, etc. The gasifier shell was rolled by a thin steel plate, and the inside gasifier was laid by fire-resistant and heat-insulating materials. The internal structure of the gasifier proper used a double-cone structure, the upper cone was shrinking to meet the characteristics of volume reduction of biomass material after gasification, and the down cone was divergent for facilitating biomass falling; the double-cone structure is beneficial to form mass flow for gasification material inside the gasifier, thus efficiently avoiding the bridge tendency of biomass material. To facilitate the users, an automatic ignition device and a butterfly valve manual ash dump device were also designed in the gasifier. The automatic ignition device was located in the center of the down cone; it consisted of an electrical heating wire connected with iron sheathing pipe; 3 layers of air distribution vents were uniformly distributed in the peripheral direction of the pipe, an iron cone brim with a larger diameter was designed at the top of the pipe to prevent the ash from blocking the air vents. Because there were also 6 tangential air inlets uniformly opened in the middle of the down cone and cooperation with the air vents on the middle pipe, a uniform air distribution could be achieved inside the gasifier. During or after an operation process, ash could be discharged into the ash hopper in time by manually rotating the butterfly valve, thus preventing its excessive deposition blocking the tangential air inlets and air vents. Temperature monitoring and gas sampling was

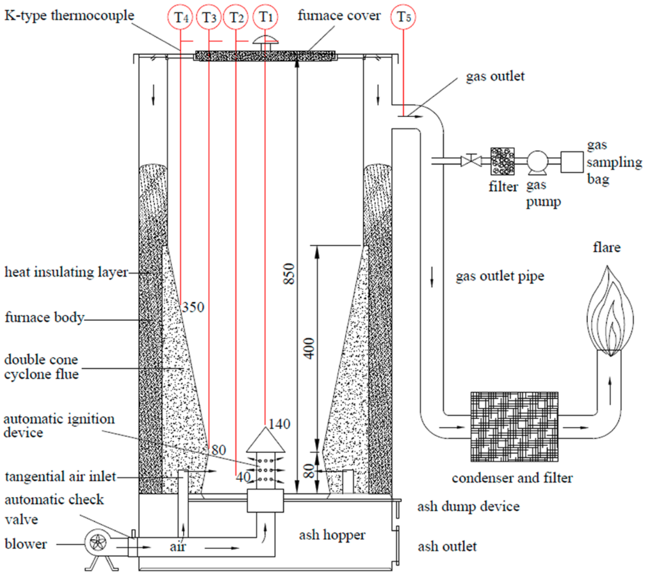

Figure 1. Schematic diagram of the updraft biomass gasifier.

designed as a whole system; it was assembled by sheathed thermocouples and a gas sampling tube through thread connection. Punching was done at the bottom of the tube to facilitate temperature measurement and gas sampling, and the product gas at different heights could be sampled using a gas pump at the top of the sampling tube as schematically shown in Figure 1. The sheathed thermocouples contained 4 K-type thermocouples with radial distribution inside the gasifier and 1 K-type thermocouple in the product gas outlet. The initial effective height of 4 thermocouples marked as 1′, 2′, 3′, and 4′ were 140, 40, 80, and 350 mm inside the gasifier, respectively, and they could also move up and down to measure the temperature and sample product gas at different heights. The internal and outlet gas temperature of the gasifier and product gas composition could be detected together in real time by this system.

The basic parameters of the gasifier were listed as follow: The gasifier is in cylindrical shape, the total height is 1000 mm, and the effective height is 850 mm except for the ash hopper. The height of the down cone and upper cone is 80 and 400 mm, respectively, the throat diameter of the double-cone proper is 220 mm, the bottom diameter is 250 mm, and the upper diameter is 380 mm, which could load more biomass material to extend the gasification time. The sheathing pipe diameter of the ignition device is 55 mm, and the iron cone diameter is 75 mm.

2.3. Experimental Method. During the experiment, the temperature of the gasifier was detected and recorded in real time. In the product gas outlet, through a connection gas sampling system as seen in Figure 1, after filtering the moisture and tars the product gas was collected using a gas sampling bag and then analyzed with gas chromatography (GC, Agilent 3000, Germany, Agilent Technologies Inc.). The detailed experimental procedure was described as follows.

Before the test, wood materials were packed into the gasifier (total capacity of ~8.9 kg) and the initial temperature of the thermocouples was recorded. Then the electrical ignition switch was turned on, after 30−40 s, the blower was opened to send air into the gasifier, and the air flow rate was adjusted by a control valve to make sure the air supply is at constant flow rate. Meanwhile, the temperature changes of the gasifier were recorded in real time. Product gas could be ignited in ~4 min generally, and the gasification condition could be checked through the combustion flame. After each test the blower was shut down to close the gasifier and the atmospheric valve was opened fully for emptying.

3. RESULTS AND DISCUSSION

3.1. Effect of Air Flow Rate on the Gasifier.

For the updraft gasifier, the operation condition is mainly adjusted by regulating the air flow rate entering into the gasifier. The air flow rate is the most important parameter during the actual operation process of the gasifier. It is closely related to the temperature distribution of the gasifier, product gas composition, and LHV.[17] Figure 2 shows the temperature of the oxidation zone (measured by thermocouple 2′ as shown in Figure 1) and gasification intensity under different air flow rates. Each temperature chosen here was under steady-state condition. During the gasification process, the main gas products are H_2, N_2, CH_4, CO, CO_2, C_2H_4, C_2H_6, C_3H_6, and C_3H_8. The profiles of gas production, gas production to air ratio, and air to fuel ratio under different air flow rates are shown in Figure 3. In addition, the product gas composition and LHV distribution under different air flow rates are shown in Table 2.

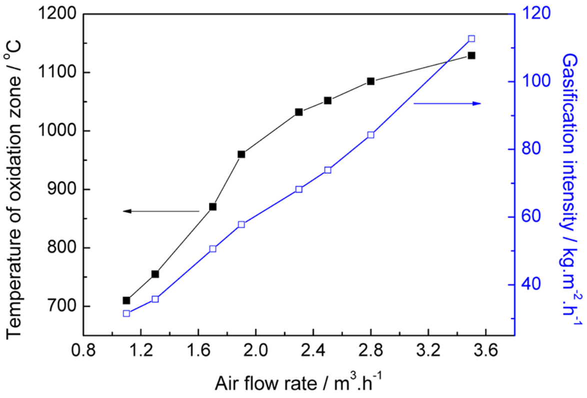

Figure 2. Temperature of the oxidation zone and gasification intensity under different air flow rates.

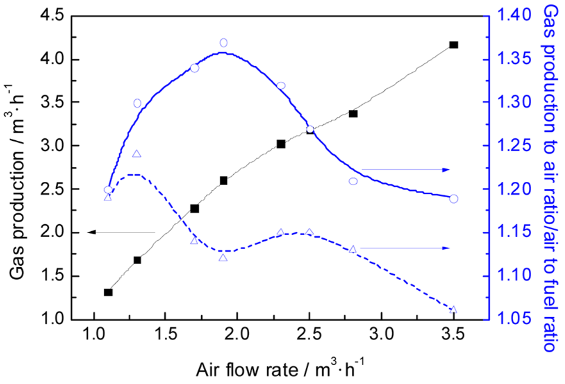

Figure 3. Gas production, gas production to air ratio, and air to fuel ratio under different air flow rates.

As seen from Figure 2, with the air flow rate increasing from 1.1 to 3.5 m^3/h the temperature of the oxidation zone increased sharply from 710 to 1129 °C and the gasification intensity enhanced largely from 31.5 to 112.7 kg/(m^2·h), thus verifying that the temperature of the oxidation zone could directly reflect the intensity of the gasification process. Considering the ash fusion point of the woody biomass used in the experiment is ~1100 °C, the air flow rate chosen for this gasifier should not exceed 3.5 m^3/h. In addition, an air flow rate of 1.7−2.3 m^3/h might be the appropriate flow rate range due to the proper oxidation zone temperature and gasification intensity. Besides, it was also demonstrated by the better LHV of the product gas of 3.83−4.38 MJ/m^3 at this range of air flow rates as shown in Table 2. From Figure 3 it can be observed that the air to fuel ratio was between 1.06 and 1.24, while gas production increased linearly with air flow rate increasing. It might be attributed to the enhanced gasification reaction and increased air flow rate. Besides, more air entered into the gasifier, more biomass would be reacted, the temperature level of the gasifier increased up to the axis space of each zone inside the gasifier expanding, and hence gas production increased. However, there was an obvious inflection (at 1.9 m^3/h) in the curve of the ratio of gas production to air flow rate. It is also shown in Figure 2 (temperature increasing rate) and Table 2 (changing trend of combustible gas content and LHV). This might indicate that there was an optimal air flow rate to get the appropriate temperature level of the gasifier, better space distribution of each zone inside the gasifier, and stable and high-efficiency gasification reaction. At lower air flow rates (e.g., 1.1 m^3/h), the temperature of the oxidation zone was very low (710 °C); hence, biomass could not be fully oxidized by air entering into the gasifier in limited contact time, thus resulting in a high content of O_2 in the product gas as shown in Table 2. Meanwhile, reactions in the reduction zone and pyrolysis zone were also weakened due to the lower temperature in each zone; hence, a lower combustible gas (H_2, CO and hydrocarbon, etc.) content was generated. Whereas with increasing air flow rate,

Table 2. Product Gas Composition and LHV Distribution under Different Air Flow Rates

air flow rate (m^3/h)	H_2	O_2	N_2	CH_4	CO	CO_2	C_{2+}	LHV (MJ/m^3)
	product gas composition (vol %)							
1.1	6.18	5.92	64.90	1.16	6.77	12.07	0.31	2.15
1.3	12.78	3.64	59.94	1.78	9.27	12.13	0.46	3.50
1.7	12.66	1.98	57.74	2.11	12.87	12.16	0.48	4.07
1.9	13.07	1.24	56.81	1.79	15.58	10.98	0.53	4.38
2.3	10.94	2.42	59.27	1.97	12.38	12.47	0.55	3.83
2.5	8.92	2.89	61.24	1.41	9.54	13.89	0.50	3.01
2.8	7.37	3.20	64.60	1.57	11.47	11.40	0.39	3.07
3.5	7.58	6.72	65.47	1.46	10.20	8.29	0.28	2.82

the temperature of the gasifier increased, the intensity of the gasification reaction in each zone was enhanced; hence, the combustible gas content in the product gas and the LHV of the product gas increased. However, with air flow rate increasing further (>1.9 m^3/h), the temperature of the gasifier was too high and the residence time of air/O_2 was too short to be fully reacted as shown in Table 2; each zone inside the gasifier expanded too much and moved up fast, the operation condition of the gasifier turned worse, and so the content of the combustible gas in the gas products decreased and the LHV of the gas products decreased rapidly.

From the above analysis, it can be obtained that an air flow rate of 1.9 m^3/h might be the optimal condition for the gasifier as it showed the highest LHV and proper temperature of the oxidation zone. In the following study, an air flow rate of 1.9 m^3/h was chosen as a typical operation condition to investigate the distribution of temperature and product gas components of the gasifier.

3.2. Temperature and Product Gas Distribution of the Gasifier at Different Running Times. Temperature and gas composition are two important parameters to understand the operation conditions of the gasifier. The temperature distribution of the gasifier at different running times is shown in Figure 4, and the gas products and LHV at different running times are shown in Table 3. According to the variation of temperature level inside the gasifier and characteristics of gas produced, the entire operation process of the gasifier could be divided into 4 parts: startup (0−4 min), transition stage (4−25 min), stable condition (25−85 min), and deteriorated condition (>85 min) as shown in Figure 4. During the startup stage, the temperature of the oxidation zone enlarged rapidly from ambient temperature to 560 °C in 4 min, the gas products could be ignited already, and the LHV of the gas products achieved 3.01 MJ/m^3. However, the gas products still contained a high content of O_2 (4.89%) and incombustible gas (N_2, CO_2, etc.). It might be attributed to the fact that the air entering the gasifier could not be completely consumed at low temperature. The transition stage was defined as the period from gas products ignition to stable operation. Moving into the transition stage, the temperature of the oxidation zone first increased largely from 560 to ~960 °C and then remained stable basically. The overall temperature level insider the gasifier rose sharply as proved by the temperature of the 1′ and 3′ thermocouples, the gasification reaction intensified, the O_2 content declined greatly from 4.89% to 1.83%, and the combustible gas content (H_2, CO, CH_4, C_{2+}) increased. It might be attributed to the fact that reactions in the reduction zone and pyrolysis zone were enhanced as a result of increasing gasifier temperature. In addition, it should be noted that because of the different distances to the oxidation zone and the furnace wall, the heating rate and response time of different parts showed a great difference which represented each thermocouple showing different heating characteristics. As running time increasing further, the temperature inside the gasifier reamined stable relatively, the space of each reaction zone was fully developed, and the gasification process moved into stable condition. Under stable condition, gas products were burned well, the combustible gas content was high, while the O_2 content remained lower, and the LHV of the product gas was larger than 4 MJ/Nm^3; moreover, it had a maximum value of 4.38 MJ/m^3 as running time at 45 min. As in the transition stage and stable condition, gas products could be both ignited and burned well and the transition stage and stable condition were also called normal operation condition. However, after ~85 min, gas products combustion turned worse and it was also observed that the temperature of the 4′ thermocouple (effective height of 350 mm, near the furnace wall) increased rapidly and the temperature variation range of the other thermocouples increased. It indicated that the temperature of the upper space of the gasifier increased, the position of each zone moved up, and the gasification condition deteriorated gradually. It can be also proved in Table 3, when running time is larger than 85 min, that the combustible gas content and LHV of the gas products decreased remarkably. Further study should be carried out to extend the use time of the gasifier.

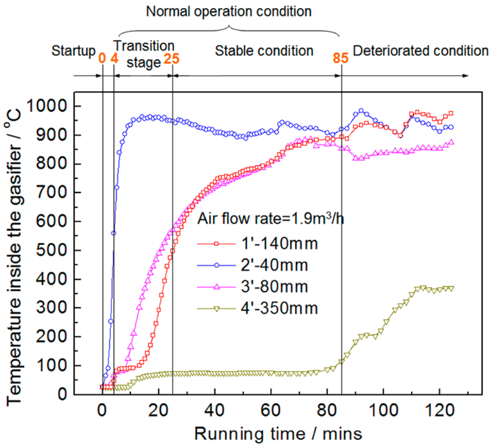

Figure 4. Temperature distribution of the gasifier at different running times.

The superficial velocity (hearth load) of the gasifier is one of the most important measures of its performance, controlling gas production rate, gas energy content, fuel consumption rate, power output, and char and tar production rate. It was defined

Table 3. Gas Products and LHV at Different Running Times (air flow rate of 1.9 m^3/h)

running time (min)	H_2	O_2	N_2	CH_4	CO	CO_2	C_{2+}	LHV (MJ/m^3)
	product gas composition (vol %)							
4	7.58	4.89	64.54	1.88	9.27	11.33	0.51	3.01
10	10.15	2.45	61.43	2.01	11.23	12.17	0.56	3.62
25	12.54	1.83	58.24	2.32	11.93	12.63	0.51	4.04
45	13.07	1.24	56.81	1.79	15.58	10.98	0.53	4.38
60	13.23	1.57	57.04	1.59	16.02	10.21	0.44	4.24
75	13.34	1.83	57.21	1.28	16.17	9.89	0.28	4.13
90	12.49	2.04	58.19	1.22	14.72	11.03	0.31	3.85
120	10.24	2.96	62.69	1.13	9.73	12.86	0.39	3.01
150	10.32	4.76	64.41	0.93	8.86	10.40	0.32	2.78

as the ratio of gas production rate to cross-sectional area.[18] Another important parameter, the turn down ratio, was defined as the ratio of the highest practical gas production rate to the lowest practical rate,[18] and it could also reflect the performance of the gasifier in a certain degree. On the basis of N balance, the superficial velocity and turn down ratio of this gasifier were calculated as 0.019 m/s and 1.32, respectively.

3.3. Temperature and Product Gas Distribution of the Gasifier at Different Heights.

To further improve the performance, the gasification mechanism of the updraft gasifier should be understood in depth. Thus, the distribution of the temperature and product gas components at different height sections has been tested to conclude the possible reaction happened inside the gasifier and seek a way to upgrade the gasifier performance, while the current work[9,18−20] mainly focuses on the operation characteristics of the gasifier.

The profile of the temperature distribution (measured by thermocouple 2′) of the gasifier at different heights is shown in Figure 5, and the gas composition and LHV of the gas products at different heights are shown in Table 4. It can be observed that the temperature decreased greatly with increasing effective height; after the height was larger than 480 mm, the temperature changed slightly; it was also found that the reaction type inside the gasifier has obvious height level characteristics. Therefore, according to the temperature distribution and reaction characteristics insider the gasifier, the internal zone of the gasifier could be divided into 4 parts: oxidation zone, reduction zone, pyrolysis zone, and desiccation zone. The typical temperature range of each zone was defined as >800, 600−800, 250−600, and <250 °C, respectively. Then the height of each zone could be calculated approximately as 130 mm, 95 mm, 195 mm, and the rest of the material height, respectively, as shown in Figure 5.

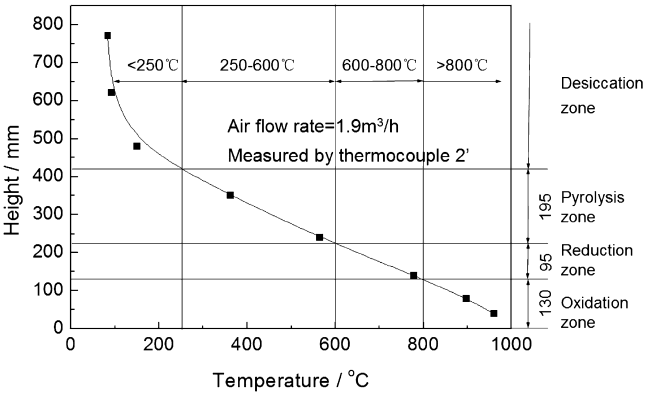

Figure 5. Temperature distribution of the gasifier at different heights.

To further analyze the gasification mechanism of the gasifier, comprehensive considering the distribution characteristics of the gas products components as shown in Table 4, the main reactions in each zone could be concluded as follows.

Oxidation zone

$$C + O_2 = CO_2 \tag{1}$$

$$C + 0.5O_2 = CO \tag{2}$$

$$CO + 0.5O_2 = CO_2 \tag{3}$$

Reduction zone

$$C + CO_2 = 2CO \tag{4}$$

$$C + H_2O = CO + H_2 \tag{5}$$

$$C + 2H_2O = CO_2 + 2H_2 \tag{6}$$

$$CO + H_2O = CO_2 + H_2 \tag{7}$$

$$C + 2H_2 = CH_4 \tag{8}$$

$$CO + 3H_2 = CH_4 + H_2O \tag{9}$$

Table 4. Product Gas Composition and LHV Distribution at Different Heights (air flow rate of 1.9 m^3/h)

height (mm)	H_2	O_2	N_2	CH_4	CO	CO_2	C_{2+}	LHV (MJ/m^3)
	product gas composition (vol %)							
40		6.05	78.52		0.16	15.27		0.02
80		1.62	74.26	0.05	7.68	16.39		0.99
140	6.38	1.46	66.75	0.21	11.82	13.38		2.26
240	11.21	1.37	60.13	1.42	13.65	11.98	0.24	3.61
350	12.36	1.3	58.21	1.65	14.45	11.58	0.45	4.05
480	13.02	1.25	57.01	1.74	15.6	10.87	0.51	4.34
850	13.07	1.24	56.81	1.79	15.58	10.98	0.53	4.38

Pyrolysis zone

$$\text{biomass} \rightarrow \text{CO} + \text{CO}_2 + \text{H}_2 + \text{CH}_4 + \text{C}_{2+} + \text{char} + \text{tar} + \text{etc} \qquad (10)$$

From Table 4 it can be observed that with increasing effective height the O_2 content in the updraft gas decreased rapidly and the combustible gas increased greatly. At different heights, the layered characteristic of the reaction type was very obvious. In the oxidation zone, at a height of 40 mm, the content of O_2 was excessive, woody material was fully combusted with a large amount of CO_2 evolving out (reaction 1), and a lot of heat was released to make the temperature of the oxidation zone up to ~960 °C. As the height increased to 80 mm, mainly because of reaction 2, the content of O_2 decreased sharply and the content of CO increased greatly with a little CH_4 generation. It should be noted that the heat from the oxidation reaction provided the whole heat demand of the other reaction zones, and heat was transferred by the updraft hot gas. Moving into the reduction zone, as the height increased further to 140 mm, the content of H_2 and CO increased significantly, the content of CH_4 increased slightly, while the content of N_2 and CO_2 decreased remarkably. It might be attributed to the fact that the hot gas from the oxidation zone reaction with the char resulted in combustible gas (CO, H_2, etc.) generation (reactions 4−9). In the pyrolysis zone, as the height reaches 240 mm, the content of H_2 and CH_4 increased remarkably, the content of N_2 continued largely decreasing, the variation of the CO and CO_2 content was reduced, and the trace C_{2+} occurred by reaction 10. Thus, reactions 5−10 might be the main reactions occurring between 140 and 240 mm. As the height increased further, the pyrolysis reaction (reaction 10) continued. When the height reached 480 mm (temperature of 150 °C as shown in Figure 5), the gas composition and LHV of the dry gas products were consistent with the outlet gas. In addition, due to the low temperature of the outlet gas (variation from 72 to 78 °C (measured by thermocouple 5′) under stable condition), tar condensation was also found in the outlet gas tube and could not be fully filtered by biomass material layer; therefore, during the actual process, material height would be right and the product gas should be used nearby.

4. CONCLUSIONS

In this paper, the temporal and spatial variation of temperature and product gas components inside the updraft biomass gasifier were studied and the relationship between it and chemical reaction was also analyzed. It was found that the air flow rate directly affects the gasification temperature and operation condition. The optimum air flow rate was at ~1.9 m^3/h, with a maximum LHV of product gas of 4.38 MJ/Nm^3 and suitable temperature of oxidation zone of 960 °C. The time of the gasifier startup and normal operation was about 4 and 81 min, respectively. In addition, different heights showed obvious layers characteristic of reaction type.

■ AUTHOR INFORMATION

Corresponding Author

*Phone: +86-27-87542417-8211. Fax: +86-27-87545526. E-mail: yhping2002@163.com.

Notes

The authors declare no competing financial interest.

■ ACKNOWLEDGMENTS

The authors express great appreciation of financial support from “Key Projects of National Fundamental Research Planning” (National 973 project 2013CB228102), the National Natural Science foundation of China (51021065), the National Key Technology R&D Program in the 12th Five Year Plan of China (2011BAD15B05-03), and the China Postdoctoral Science Foundation (2012M521425).

■ REFERENCES

(1) Huang, H.; Gao, N. *Energy Procedia* **2011**, *5*, 2137−2141.

(2) Xinhua 2009; http://news.xinhuanet.com/english/2009-12/12/content_12633683.htm.

(3) Abdelaziz, E. A.; Saidur, R.; Mekhilef, S. *Renewable Sustainable Energy Rev.* **2011**, *15*, 150−168.

(4) Lu, X.; Yu, Z.; Wu, L.; Yu, J.; Chen, G.; Fan, M. *Fuel Process. Technol.* **2008**, *89*, 475−484.

(5) China-Briefing, 2012; http://www.china-briefing.com/news/2012/08/24/china-releases-12th-five-year-plan-for-energy-saving-and-emission-reduction.html.

(6) Beenackers, A. A. C. M. *Renewable Energy* **1999**, *16*, 1180−1186.

(7) Okuga A. Analysis and operability optimization of an updraft gasifier unit. M.S. Thesis, Dept. Mech. Engineering, Eindhoven University of Technology, Eindhoven, Netherlands, 2007.

(8) Ueki, Y.; Torigoe, T.; Ono, H.; Yoshiie, R.; Kihedu, J. H.; Naruse, I. *Proc. Combust. Inst.* **2011**, *33*, 1795−1800.

(9) Chen, W.; Annamalai, K.; Ansley, R. J.; Mirik, M. *Energy* **2012**, *41*, 454−461.

(10) Liu, H.; Hu, J.; Wang, H.; Wang, C.; Li, J. *J. Nat. Gas Chem.* **2012**, *21*, 374−380.

(11) Kayal, T. K.; Chakravarty, M.; Biswas, G. K. *Bioresour. Technol.* **1994**, *49*, 61−73.

(12) Vittorio T.; Giorgio C. Process analysis and performance evaluation of updraft coal gasifier. In *Proceedings of the 3rd International Conference on Clean Coal Technologies for Our Future*; Sotacarbo, IEA Clean Coal Center, IEA, Sardinia, Italy, 2007.

(13) Murgia, S.; Vascellari, M.; Cau, G. *Fuel* **2012**, *101*, 129−138.

(14) Higman, C.; Van der Burgt, M. *Gasification* **2008**, *10*, 87−97.

(15) Prins, M. J.; Ptasinski, K. J.; Janssen, F. J. J. G. *Energy* **2007**, *32*, 1248−1259.

(16) Raveendran, K.; Ganesh, A.; Khilart, K. C. *Fuel* **1995**, *74*, 1812−1822.

(17) Yang, S.; Xue, Y.; Niu, G. *Energy Conserv. (China)* **2009**, 6−9.

(18) Saravanakumar, A.; Haridasan, T. M.; Reed, T. B.; Bai, R. K. *Fuel* **2007**, *86*, 2846−2856.

(19) Saravanakumar, A.; Haridasan, T. M.; Reed, T. B.; Bai, R. K. *Fuel Process. Technol.* **2007**, *88*, 617−622.

(20) Saravanakumar, A.; Haridasan, T. M.; Reed, T. B.; Bai, R. K. *Energy Sustainable Dev.* **2005**, *9*, 25−39.